Water Ingress Detection in Low-Pressure Gas Pipelines Using Distributed Temperature Sensing System

Wang, Libo; Narasimman, Srivathsan Chakaravarthi; Ravula, Sugunakar Reddy; Ukil, Abhisek

2016

Wang, L., Narasimman, S. C., Ravula, S. R., & Ukil, A. (2016). Water Ingress Detection in Low-Pressure Gas Pipelines Using Distributed Temperature Sensing System. IEEE Sensors Journal, 17(10), 3165-3173.

https://hdl.handle.net/10356/81609

https://doi.org/10.1109/JSEN.2017.2686982

This article has been accepted for publication in a future issue of this journal, but has not been fully edited. Content may change prior to final publication. Citation information: DOI 10.1109/JSEN.2017.2686982, IEEE Sensors Journal

Water Ingress Detection in Low-Pressure Gas Pipelines Using Distributed Temperature Sensing System

Libo Wang, Srivathsan Chakaravarthi Narasimman, Sugunakar Reddy Ravula, and Abhisek Ukil, *Senior Member, IEEE*

***Abstract*—In a distribution network of low-pressure gas pipelines, the situation of gas leak can be further aggravated when groundwater enters the pipeline through leaks and eventually blocks the gas flow. This will have critical implications on the gas supply to the customers. This is termed as 'water ingress', which typically happens only in low-pressure distribution networks, and not in high-pressure transmission networks. In order to find the location of water ingress, distributed temperature sensing (DTS) system has been used experimentally. The results show significant temperature change immediately after the onset of water ingress, and with data post-processing based on temporal difference, location information of the leak can be obtained. With a selected time window of interest, the inclination of gas pipeline is also indicated by the differenced temperature profiles. The DTS system is still capable of identifying the position, even if the location of water ingress is changed.**

***Index Terms*—Distributed network of low-pressure gas pipeline, water ingress detection, distributed temperature sensing (DTS) system, temporal difference, gas network condition monitoring.**

I. Introduction

IN OIL/GAS industries, the most effective way to transport and distribute natural gas or town gas is through gas pipeline networks, which can be classified into two categories: transmission network and distribution network. The transmission network is operated under high pressure (e.g., 28–40 bar), while the operating pressure of the distribution network is at medium (e.g., 3–5.5 bar) and low range (e.g., 2–50 kPa). Compared to the transmission network, the distribution network is longer and more complex. For instance, the gas distribution network in Singapore is more than 3000 km in length, which is 10 times longer than the transmission network [1].

One of the major downfalls of gas pipelines is leak which can be caused by corrosion of pipes, loosening of joints, or third-party damages. Leaks can have critical implications particularly in the case of the distribution network since they are found predominantly in the residential areas. This is further aggravated in the case of low-pressure underground pipelines, wherein groundwater enters the pipeline through the leaks. This eventually blocks the flow of gas, or even causes internal corrosion, which is known as water ingress problem [2], [3]. The water ingress in pipelines typically cannot be detected until the pipeline is completely blocked by water and the users complain about the lack of gas supply, which could be days after the onset of the problem. This is an extremely inefficient solution to the problem since the exact position of the water ingress would not be known even after the customer has been discomforted. According to SP Group's (known as Singapore Power prior to Feb 2017) report, there are annually more than 25 water ingress related problematic cases in their gas pipeline distribution network [1], which requires robust detection and monitoring technology.

In our previous report [4]–[6], a pressure and flow sensor-based monitoring system has been proposed to identify the leak and water ingress in the low-pressure gas pipeline. It clearly shows that when water ingress occurs, the gas pressure starts to oscillate and the magnitude of oscillation increases with the amount of water injected, even when the initial gas pressure is as low as 2 kPa. However, the oscillation in gas pressure only shows the occurrence of water ingress rather than the location. It has been found that there is a marked difference between the temperature of the pipeline and the temperature of the water that leaks into the pipeline. This difference in temperature can be used to detect the point of water ingress into the pipeline. Therefore, in this work, a new method based on temperature detection has been employed to experimentally study the water ingress problem. The monitoring system is based on the technology of distributed temperature sensing (DTS) which uses optical fiber as the temperature sensor.

DTS systems have been developed significantly since they were firstly conceptualized in 1980s [7], [8]. In the past decades, DTS systems have become capable of measuring temperature with high accuracy over a long distance, which makes it very suitable for monitoring oil/gas pipelines [9]–[11]. Nowadays, DTS systems have been used in many applications, such as electrical power system, building monitoring, equipment monitoring, etc. [12]–[16]. To the best of our knowledge, it is the first time that DTS system is used for investigating water ingress problem in low-pressure gas pipelines, even though DTS has been applied at high-pressure gas pipeline leak detection. However, the problems in the low- and high-pressure regimes in gas pipelines are quite different

This work is supported by the energy innovation programme office (EIPO) through the national research foundation and Singapore energy market authority. Project LA/Contract No.: NRF2014EWT-EIRP003-002.

Libo Wang, Srivathsan Chakaravarthi Narasimman, and Sugunakar Reddy Ravula are with the Energy Research Institute (ERI@N), Nanyang Technological University, Singapore, (email: libo@ntu.edu.sg; srivathsan.cn@ntu.edu.sg; sugunakar@ntu.edu.sg).

Abhisek Ukil is with the School of Electrical & Electronic Engineering, Nanyang Technological University, Singapore, (email: aukil@ntu.edu.sg).

This article has been accepted for publication in a future issue of this journal, but has not been fully edited. Content may change prior to final publication. Citation information: DOI 10.1109/JSEN.2017.2686982, IEEE Sensors Journal

in nature.

The remainder of the paper is organized as follows. Section II presents the evaluation of DTS system as well as the method that has been used for data processing. Section III describes the details of the experimental setup and test procedures. The experimental results have been presented and discussed in Section IV, followed by conclusions in Section V.

II. Evaluation of DTS System and Method

A. Fundamentals of DTS system

The optoelectronic devices, called distributed temperature sensors (DTS), utilize optical fiber as linear sensors for temperature measurement over a long range of distances. Compared to the traditional point temperature sensors, linear sensors with thousands of points can realize continuous reading along the entire length and provide a continuous temperature profile within a short period of time. The commercial DTS systems are capable of measuring temperature with the high accuracy of 0.01 ^{o}C and achieve high spatial resolution of 1 m over the distance up to 30 km [13].

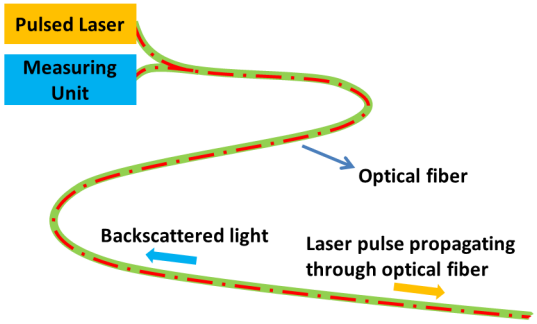

Fig. 1: Principle of DTS system based on OTDR technique.

The distributed temperature sensing system used in this work is based on Optical Time-Domain Reflectometry (OTDR) technique, as shown in Fig. 1. In general, as a laser pulse is emitted from the source and propagates through the fiber core, a small part of light travels back due to scattering effect. Compared to the laser source with only one peak on its spectrum, the properties of backscattered light have been changed with three main components and five broad bands shown in Fig. 2 [17]. Generally, Raman scattering is only sensitive to temperature, while Brillouin scattering is sensitive to strain as well [18], [19]. For either temperature or strain, the physical changes will affect the material properties of the optical fiber and change the feature of interaction with the pulsed laser, which results in changes of intensity and/or wavelength shift in the spectrum through Stokes and anti-Stokes processes. For Raman scattering, only the anti-Stokes component rather than the Stokes component is affected when the temperature varies. The temperature information can be derived from the intensity ratio of anti-Stokes to Stokes signals [20], which usually gives very high temperature resolution in the order of 0.01 ^{o}C.

The location information of the temperature profile is obtained from the measuring technique based on the time of flight. As the velocity of light in the optical fiber is constant, the return time for a laser pulse from the laser source to a certain point is determined only by the distance on the cable. The parameter, known as spatial resolution, is defined as the distance between the positions where 10% and 90% of temperature response to a step change introduced in a system are observed, as shown in Fig. 3. Each point corresponds to one temperature reading and the constant distance between two such points is also known as sampling resolution or sampling interval. Typically, the sampling interval could be 2-5 times smaller than the spatial resolution.

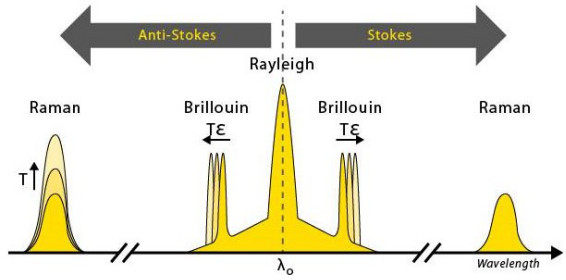

Fig. 2: Schematic spectrum of backscattered light, intensity vs. wavelength.

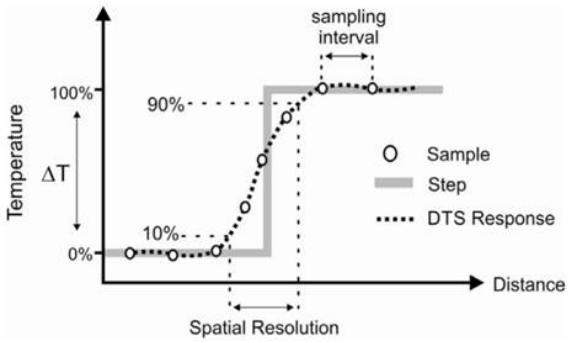

Fig. 3: Example of DTS spatial resolution defined by temperature step.

Another parameter to be considered is the measurement time, which refers to the time required to take one set of readings of a temperature profile from one channel of the DTS. The measurement time depends on several factors, such as temperature resolution, spatial resolution, fiber length and signal processing capability of backscattered light. Generally, the default minimum measurement time is in the order of seconds, and typically set by the DTS manufacturer. Increasing the measurement time will lead to better resolution for temperature and/or spatial measurements, which makes it suitable for a wide variety of applications.

The advantages of optical fiber based DTS include immunity to electromagnetic interference, insensitivity to humidity and corrosion, no requirement for active electronic circuits, long term reliability and intrinsic safety for use in hazardous environments. Thus, the demand for DTS systems keeps increasing in some industrial applications, especially in harsh environments [14], [15], [21], [22].

This article has been accepted for publication in a future issue of this journal, but has not been fully edited. Content may change prior to final publication. Citation information: DOI 10.1109/JSEN.2017.2686982, IEEE Sensors Journal

B. Experimental evaluation of DTS temperature reading with minor contact

The DTS system used in this work was the Oryx SR from Sensornet, which requires only a 12-24V DC power supply. The built-in laser is a semiconductor laser with wavelength of 975 nm and average output power less than 1.5 mW. This model of DTS comes with 4 channels and is suitable for either one-end or double-end configuration. It also features a spatial resolution of 1 m with sampling resolution of 0.5 m and temperature resolution as good as 0.01 ^{o}C. The maximum measuring range covers up to 5 km, while the minimum measuring time is as low as 10 s [23].

For some applications with objects installed above the ground, the applied DTS sensing cable is fixed on the body with minor contact and the rest of sensing cable surface is exposed to air. To evaluate the influence of ambient temperature on the DTS temperature reading, an experimental test was carried out by attaching the sensing cable onto the surface of a metal gas pipe. The ambient temperature of the place surrounding the DTS cable was measured using a resistance temperature detector (RTD) and named as T_{ambient}. The temperature of the metal pipe beside the DTS cable was measured by an infrared (IR) thermometer and named as T_{pipe}. The temperature reading from the DTS system was labeled as T_{DTS}. Fig. 4 shows the schematic diagram of the positions from which the three different temperature readings were taken. The measurements were taken on two different days: one was sunny and the other was cloudy. Total length of the temperature measurement performed was more than 1 m as the spatial resolution of DTS system is 1 m.

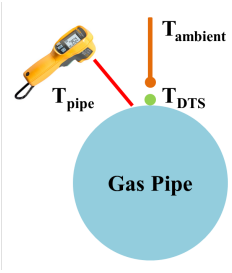

Fig. 4: Schematic diagram of different temperature measurement techniques for comparison.

All the temperature readings are summarized in Table I, represented as mean temperature and the corresponding temperature distribution. It can be seen that for the sunny day, the values of T_{DTS} and T_{pipe} were very close, while T_{ambient} that was measured by the RTD was lower. This is because the metal pipe is heated up by absorbing the energy from sun light. However, for the cloudy day, all the three temperature readings were similar as the testing area reached thermal equilibrium and heat exchange between metal pipe and environment was not significant. Therefore, it can be concluded that even with minor contact between the DTS sensing cable and the pipe surface, it is still possible to measure the temperature of the pipe using the DTS system and the influence of ambient temperature is negligible.

TABLE I
Summary of temperature readings using different approaches

Weather	Sunny	Cloudy
T_{ambient}	39.5 $\pm$ 0.4 ^{o}C	32.8 $\pm$ 0.5 ^{o}C
T_{pipe}	43.8 $\pm$ 0.5 ^{o}C	32.9 $\pm$ 0.6 ^{o}C
T_{DTS}	44.2 $\pm$ 0.3 ^{o}C	33.2 $\pm$ 0.4 ^{o}C

C. Data post-processing based on temporal difference

In order to identify the time dependent temperature change of the profile, a data processing method based on temporal difference is introduced. The temporal temperature profile difference is calculated by subtracting the temperature profiles obtained from two time instances that are Δt time steps apart. For a window of time from t_s to t_p and fixed interval time of Δt, the temporal temperature profile difference is calculated for temperature profile at every time instant. Typically, the minimum interval time is determined by the choice of measurement time. By varying the interval time from small to large value and the time window to focus on a particular point of time, it is possible to not only detect the slight changes but also observe the trends of temperature profiles and gather general information from larger sets of data.

$$\Delta T_{\text{sp}}(\Delta t) = \frac{1}{t_p - t_s} \sum_{t=t_s}^{t_p} T(t + \Delta t) - T(t), \qquad (1)$$

where, ΔT_{sp} is the mean temperature difference for the entire profile, Δt is the step change in time for which the temperature change is to be calculated, t_s is the start time index, t_p is the stop time index, and $T(t)$ is the temperature profile of the pipeline at time instant t.

Temporal differencing facilitates calculation of the time instant corresponding to the onset of water ingress in the pipeline. This becomes important for the current problem since the temperature change apart from being small is also fleeting. Therefore, analysis of temperature profiles at the time instant where water is found to have entered the pipeline is detrimental to the process of detection. Further, the temporal difference is useful to delineate the point of water ingress in cases where a marked difference is expected. When the temperature profile has a single driving factor and is not significantly influenced by disturbances the temporal differencing technique yields good results.

III. Experimental Setup & Testing Procedure

A. Test bench arrangement

The experimental tests were carried out in the test bench under SP group, Singapore. The whole test setup was placed above the ground for training and ease of operation, which can be seen from Fig. 5. The total length of test setup is about 40 m of which 9 m is DN150 ductile iron (DI) pipe and the rest is polyethylene (PE) pipe. For this project, only the DI pipe is studied since leak and water ingress are far more likely to occur in the DI pipe rather than the PE pipe and, according to the SP Group, the metallic DI pipe is still dominating the gas pipeline distribution network with percentage of 55%. The outside and inside diameters of DI pipe are 170 mm and 158 mm, respectively. Additionally, a polyethylene sleeve covers the surface of the DI pipe, protecting the metal gas

This article has been accepted for publication in a future issue of this journal, but has not been fully edited. Content may change prior to final publication. Citation information: DOI 10.1109/JSEN.2017.2686982, IEEE Sensors Journal

pipeline from corrosion in harsh environmental conditions. The schematic diagram of the section of DI pipe is shown in Fig. 6. There are mainly 2 pieces of DI pipe with lengths of 1.8 m and 5.8 m, which are connected with a flange. At each end of the pipeline, a DN150 to DN100 reducer is installed and connected to the PE pipe as one is for inlet and the other is for outlet. Gate valves are installed at both ends of the pipeline to control the gas flow from regulator to the test setup. In addition, a set of pressure (PT) and flow transmitters (FT) are installed at each port to monitor the pressure and flow rate of the live gas pipeline. In between the PTs and FTs, 3 leak valves (LV1, LV2 and LV3) are installed to simulate the leak at different positions. Moreover, from inlet to outlet, it has been found that there is a certain degree (1-3^o) of inclination, which is very common in a real gas pipeline network.

Fig. 5: Picture of experimental test setup in Singapore.

B. Installation of optical fiber cables (DTS)

Along the gas pipe from outlet to inlet in our test setup, 4 optical fiber cables starting from main unit of distributed temperature sensing (DTS) system are laid on the surface of metal pipe, which is shown in Fig. 7. For each sensing cable, a multi-mode 50/125 μm graded index optical fiber is inserted into a double-layered protection cable, which consists of one layer of plastic tubing covered with a layer of stainless steel housing (see Fig. 7). The type of optical fiber with large core allows more power of back-scattered light to be collected for Raman signal processing, which is required for long range monitoring application. The double-layered shielding effectively protects the fragile optical fiber from damage caused by third-party operations. It also makes the sensing cables suitable for applications in harsh environments. The drawback of having metal housing is that the cables lose the flexibility and become difficult to bend. All four sensing cables are respectively connected to the four channels on the DTS unit and they are labeled accordingly from channel 1 to channel 4. Channel 1 is located on the top of the gas pipe and close to the leak valves, while channel 3 is at the bottom and channel 2 and 4 are fixed on the sides of the pipe. There is a 90^o difference between consecutive cables and the entire configuration is also shown in the inset of Fig. 7.

In the current test setup, the section of the DI pipe approximately corresponds to the range from 30 m to 39 m on DTS sensing cables. The presence of flanges and reducer fittings to facilitate connection of pipes at the test setup hinders the DTS cable coming into contact with the pipe surface consistently, introducing bends in the cable which do not manifest themselves immediately due to the metal sheath on

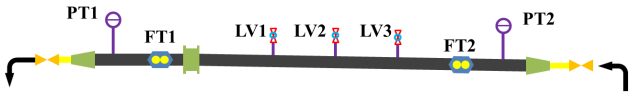

Fig. 6: Schematic diagram of the DI pipe under study.

Fig. 7: Installation of DTS sensing cables on the surface of DI pipe. Inset: view of cross section

the cable reducing the flexibility of the fiber. Hence, these fittings further reduce the effective length of the pipe that can be studied for an accurate temperature profile to 5.8 m within which all the search algorithms considered must be applied. The locations on DTS sensing cable are approximately 34.67 m, 35.64 m and 36.56 m for LV1, LV2 and LV3, respectively.

C. Water ingress tests

The water ingress tests were carried out by injecting tap water into the live gas pipeline through any one of the leak valves. The dimension of leak valve is 25 mm (1 inch) and, to simulate a small leak, a 1 mm gap was set by carefully adjusting the opening angle of the ball valve. The flow rate of water ingress was regulated by the source tap and measured by a water meter. The average flow rate was about 1.33×10^{-4} -1.66×10^{-4} cubic meters per second, m^3/s (8-10 litres per minute, LPM). The water ingress was stopped for about 3 minutes after 27 litres of water was injected. The on/off (start/stop) operation was repeated 3 times and about 81 litres of water was injected into the gas pipeline. It is worth to note that the test setup was connected to the live line via a PE pipe and all the tests were conducted under live situation. To avoid any water drifting from test bench to the live gas pipeline network, water ingress was stopped immediately after the small PE pipe was fully blocked. The temperature measurement from the DTS covers the temperature profiles before and after water ingress tests.

IV. Results and Discussion

A. Effect of environment on the temperature profile

A typical temperature profile recorded by DTS that covers the whole test bench is shown in Fig. 8 and the total length of the DTS sensing cable is about 75 m. As mentioned in Section III, the studied section of DI pipe corresponds to the distance between 30 m to 39 m on DTS cable. It can be seen that the temperature distribution varies from 33 ^{o}C to 46 ^{o}C

This article has been accepted for publication in a future issue of this journal, but has not been fully edited. Content may change prior to final publication. Citation information: DOI 10.1109/JSEN.2017.2686982, IEEE Sensors Journal

when it was sunny (Fig. 8a), while it varies from 30 ^{o}C to 33 ^{o}C when it was cloudy (Fig. 8a). However, compared to the temperature distribution from when the DTS sensing cable is buried under ground, the variation is much more significant within such a short distance. It should be attributed to the influence from the environment, such as weather (e.g., sunny, cloudy and rainy days). All the factors increase the complexity of the test setup and difficulty of conducting the experiments. On the other hand, it mimics the real environmental condition when the gas pipeline is installed above the ground.

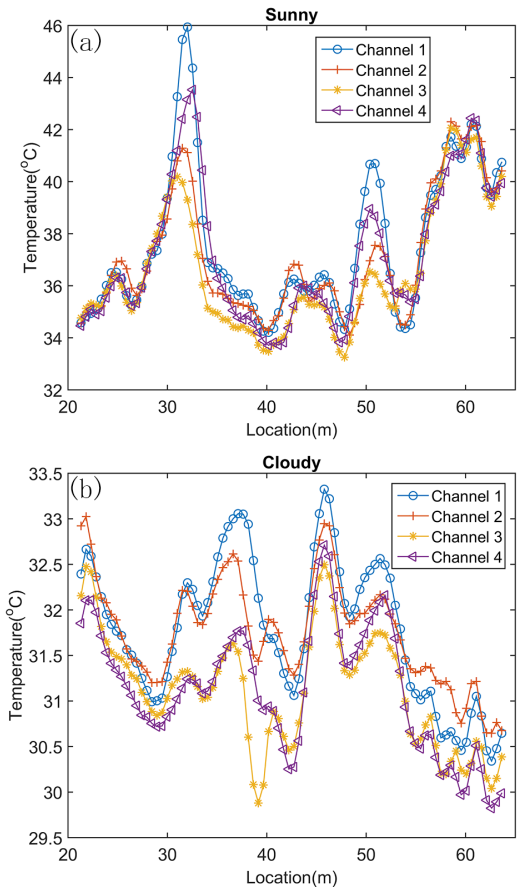

Fig. 8: Overview of temperature profiles for the whole test bench on different days: (a) sunny and (b) cloudy.

B. Analysis of water ingress tests

In case of water ingress test, water was injected manually through leak valve (LV) and due to the small inclination of the DI pipe, injected water flows towards the lower part of the pipeline, near the gas inlet port. The average temperature of injected water is about 28 ^{o}C, which is different from that of the metal gas pipeline. Due to the heat exchange between the water and pipe, the temperature of the gas pipe changes. As mentioned in previous sections, the minimum measurement time for DTS per channel is 10 s and thus, it takes at least 40 s to get one set of temperature readings for the 4 channels. However, the moment water ingress begins, the temperature change occurs rather rapidly. Hence, to improve chances of identifying the onset of water ingress, channel 1 and 3 or even channel 3 alone were used to detect the temperature change in the gas pipeline. Fig. 9 shows the variation of temperature profile from channel 3 when a typical water ingress test was carried out on LV2. All the temperature profiles were recorded with a measurement time of 10 s and an interval time of 30 s. It can be seen that at the affected area, the temperature drops by about 2 ^{o}C, which is comparable to the temperature distribution for the entire profile. Thus, it would be very difficult to identify such kind of temperature change under complex background with only one temperature profile for each time.

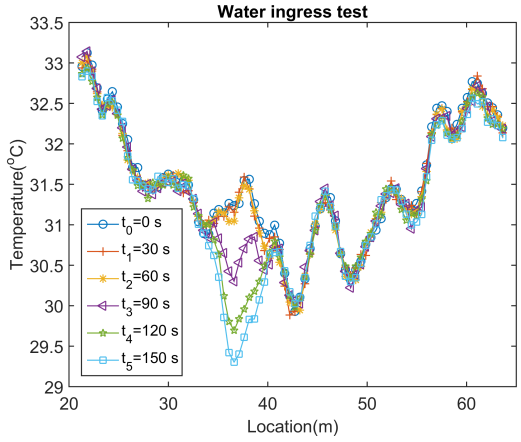

Fig. 9: Temperature profiles of water ingress test with time before and after onset.

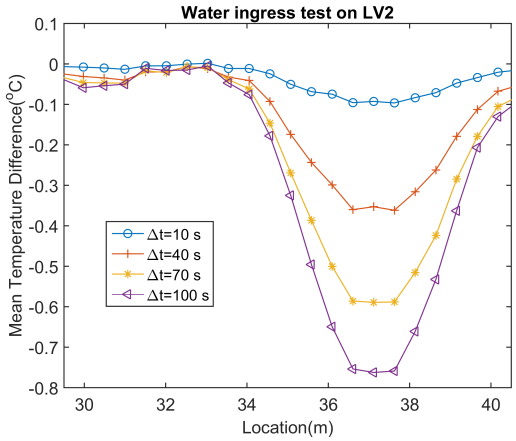

Fig. 10: Mean temperature difference ($\Delta T_{\mathrm{sp}}(\Delta t)$) where sp represents the entire span of data and different interval time of Δt from 10 s to 100 s is used during water ingress test.

As shown in Fig. 9, except the section of DI pipe, the rest of the temperature profile does not change significantly, which makes it possible to apply methods based on temporal difference for data processing with a time window that covers the entire water ingress test. With a fixed interval time (Δt), temperature change of each point along the DTS sensing cable is calculated with a different starting time and accordingly, the mean value of temperature change at each point is obtained. Focusing on the temperature profile from 30 m to 39 m and the temperature readings from channel 3 only, the results of mean temperature difference with different interval time of Δt are shown in Fig. 10. It can be seen that, for each Δt, the value

This article has been accepted for publication in a future issue of this journal, but has not been fully edited. Content may change prior to final publication. Citation information: DOI 10.1109/JSEN.2017.2686982, IEEE Sensors Journal

of ΔT_{sp} has a significant drop in the pipe section from 33 m to 39 m with the lowest point near 37 m. However, taking LV2's location at 35.64 m as a reference, the point with the maximum temperature drop is shifted away by 1.5 m. It should be attributed to the inclination of gas pipeline and because of gravity and low gas pressure, the injected water flows away from the location of leak valve toward the gas inlet port and fills up the lowest part of the test setup. Fig. 10 shows that, increasing Δt from 10 s to 100 s, causes a ten fold increase in the absolute value of ΔT_{sp} from 0.08 ^{o}C to 0.9 ^{o}C. This is due to the fact that the heat exchange requires certain time to reach the thermal equilibrium at the affected area.

C. Analysis of onset and location of water ingress

The temperature profiles observed in Fig. 9 show that the drop in temperature is significantly greater during the time instant when water enters the pipeline. This difference persists for a small window of time after which the thermal equilibrium is achieved, and there is no further observable drop in the temperature. In order to estimate the time instant that corresponds to the onset of water ingress, the maximum temperature drop between the consecutive temperature profiles corresponding to each measuring point on the pipeline is used to find the most frequently occurring time index (t). This process is repeated by varying the interval time, from 10 s to 30 s while the time index of interest and the number of times it occurs along the DTS profile is used to calculate the weighted average where the weight assigned to each individual time index (M) is the frequency of occurrence (F).

$$t = \frac{M1 \times F1 + M2 \times F2 + M3 \times F3}{F1 + F2 + F3}, \qquad (2)$$

where t is the weighted time index close to the onset of water ingress in the pipe; $M1, M2, M3$ are the time indices of maximum temperature change corresponding to interval time 10 s, 20 s and 30 s respectively; $F1, F2, F3$ are the frequencies of occurrence of the time index of maximum temperature change corresponding to interval time 10 s, 20 s and 30 s respectively.

The time instant t_0 which is the closest time index just before calculated weighted time index t is selected as the time index corresponding to the onset of water ingress test. The time window of interest is considered from 9 instances before the time instant t_0 till 4 instances after t_0. The temperature profiles recorded over this window of interest can be analyzed further and the results of mean temperature difference over a minute are shown in Fig. 11. The mean temperature difference is calculated in order to correct for the effect of transient spikes in the temperature profile.

The step change for the mean temperature data with an interval time of 10 s shows a persistent drop in temperature, in which the lowest point is found to move from 35.59 m to 37.12 m. The initial significant temperature drop is observed at the time instant t_0, in which the lowest point is 35.59 m. This is observed to be the initial contacting point that water enters into the pipeline and causes the temperature change. The actual location of LV2 as mentioned earlier is 35.64 m, which is consistent with the findings obtained from Fig. 11.

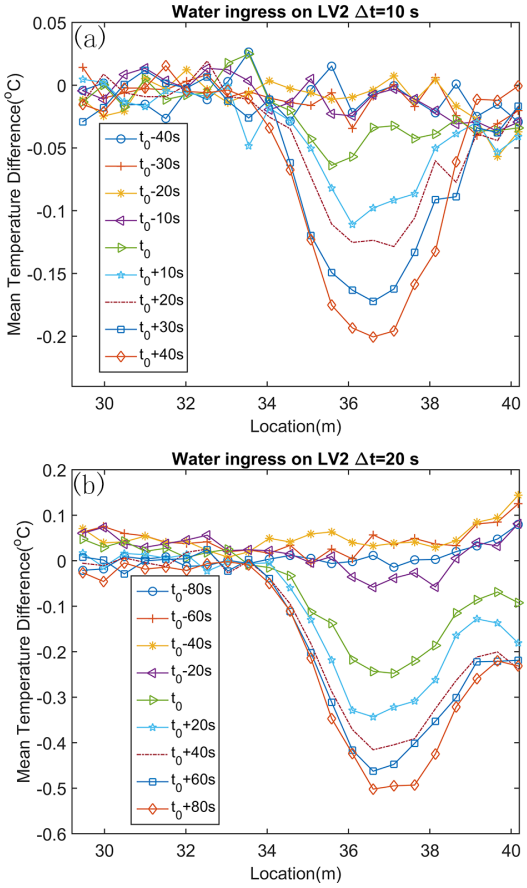

Fig. 11: Mean temperature difference ($\Delta T_{\text{sp}}(\Delta t)$) where sp covers a 60 s window with an interval time Δt of 10 s (a) and 20 s (b) during onset of water ingress.

The movement of the lowest point in the subsequent time instances occurs since the water is found to flow to the lowest point of the pipeline due to the inclination. This phenomenon is found to persist until thermal equilibrium ensues, till then the lowest point keeps moving along the same direction but the temperature difference is not as marked as is the case with the time window of interest. Compared to the results obtained from Fig. 10, location information found with 1 minute time window of interest is more accurate and the inclination of gas pipeline is also indicated. When both the channel 1 and 3 are used, the window of interest is expanded to cover twice the previous region and since data is obtained only once every 20 s the first lowest point recorded is at 36.61 m. Hence the results are observed to be better when channel 3 alone is used.

D. Analysis of water ingress tests on different locations

Water ingress tests were also carried out on LV1 and LV3 with the same experimental procedures. Following the same data processing method, the results of mean temperature difference for 1st water ingress test have been shown in Fig. 12. As water ingress test starts, it clearly shows similar mean temperature difference curves and that the lowest point of the initial temperature drop observed from DTS system agrees well with the physical location of leak valves on the sensing cable. For water ingress test on LV1 which is located

This article has been accepted for publication in a future issue of this journal, but has not been fully edited. Content may change prior to final publication. Citation information: DOI 10.1109/JSEN.2017.2686982, IEEE Sensors Journal

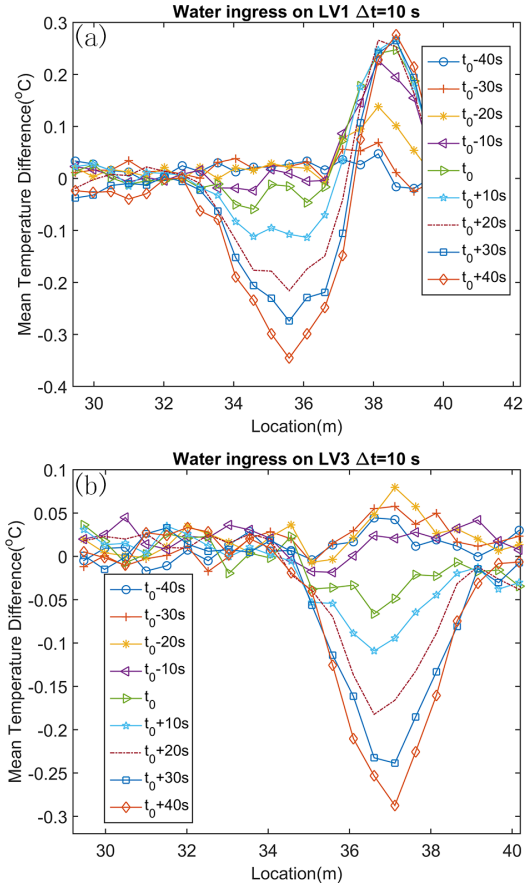

Fig. 12: Mean temperature difference ($\Delta T_{\mathrm{sp}}(\Delta t)$) where sp covers a 60 s window with interval time Δt of 10 s during onset of water ingress in LV1 (a) and LV3 (b).

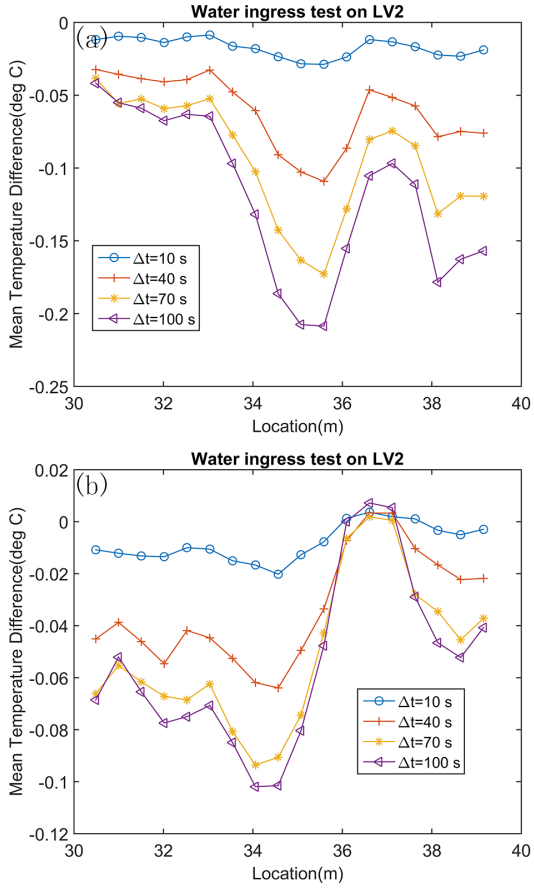

Fig. 13: Mean temperature difference ($\Delta T_{\mathrm{sp}}(\Delta t)$) where sp represents the entire span of data and different interval time of Δt from 10 s to 100 s is used for the subsequent second (a) and third (b) water ingress tests.

at 34.67 m, the obtained location information from DTS is 34.56 m which is in the range of sampling resolution of 0.5 m. Similarly, it has been found that the location of LV3 is 36.56 m and the lowest point of the initial temperature drop is at 36.61 m. Due to the inclination of gas pipeline, similar shift of lowest point in the subsequent time instances is found. For LV1 and LV2, the points of maximum temperature change are shifted by more than 1 m, while there is only 0.5 m shift in case of water ingress test on LV3. It should be attributed to the reducer fitting near the location of 39 m that partially blocks the water flow and accumulates the injected water. Hence, it can be concluded that although the spatial resolution of DTS system is 1 m, it is still possible to find the leak position with the same order of accuracy in case of water ingress. It also can be seen that the absolute temperature changes observed during tests on different leak valves varies from each other. This can be attributed to the difference in temperature offset between the water and gas pipelines.

E. Subsequent water ingress tests

To investigate the influence of water ingress when water is already inside the DI pipe, the same amount of tap water was injected after 3 minutes. For the subsequent second and third water ingress tests on LV2, the corresponding results have been shown in Fig. 13. During the tests, similar profiles of mean temperature difference are observed. However, not only the magnitudes of maximum temperature drop but also the locations have been changed. It is because the temperature difference between the gas pipe and tap water is not as large as that of first water ingress test. In addition, water level inside the gas pipe increases as water is continuously injected and the new affected area shifts from 37 m to 34 m as shown in Fig. 13. It is necessary to mention that at the location of 33 m, a flange is placed to connect two pieces of DI pipe, which causes the temperature reading within this section to deviate from the trend of temperature change during water ingress. Nevertheless, it clearly shows that with data post-processing, the measurement by DTS system is able to identify the small change during water ingress tests and provides relevant location information of water flow.

V. Conclusion

Leak in gas pipelines is one of the critical problems that companies in oil/gas industries encounter. For distribution network with low-gas pressure, the problem can be even more severe when water comes into the pipe and blocks the flow of gas. In this paper, water ingress problem on low-pressure gas pipelines has been experimentally studied using distributed temperature sensing. Although the test setup is exposed to the vagaries of the environment that makes temperature readings along the DI pipe vary significantly, it is

This article has been accepted for publication in a future issue of this journal, but has not been fully edited. Content may change prior to final publication. Citation information: DOI 10.1109/JSEN.2017.2686982, IEEE Sensors Journal

still possible to find the small temperature change by applying temporal differencing on the temperature profile. The highest single step temperature drop observed from the DTS data corresponds to the time instant of the onset of water ingress and this change can be used to detect the time window of interest which on analysis yields the leak location with better accuracy. The inclination in the pipeline can be tracked by observing the movement of the point of maximum change in temperature on the profile. The accuracy of leak localization is found to depend on the environment, the flow rate of water into the pipeline, the interval time and the time window over which the temperature profile is observed. When the water level changes slowly, the movement of water in the pipeline can be tracked. Therefore, it can be concluded that the optical fiber based DTS system is very promising for monitoring water ingress on low-pressure gas pipelines and identifying the location of the leak.

ACKNOWLEDGMENT

The authors thankfully acknowledge the technical support by the engineers of the SP group.

REFERENCES

[1] Singapore Power, whitepaper. [Online]. Available: http://www.singaporepower.com.sg

[2] G. J. Hatton, M. Pulici, G. Curti, M. Mansueto, and V. R. Kruka, "Deepwater Natural Gas Pipeline Hydrate Blockage Caused by a Seawater Leak Test," presented at the Offshore Technology Conference, Houston, Texas, 2002.

[3] E. O.-o. Obanijesu, V. Pareek, and M. O. Tade, "Hydrate Formation and its Influence on Natural Gas Pipeline Internal Corrosion Rate," presented at the SPE Oil and Gas India Conference and Exhibition, Mumbai, India, 2010.

[4] R. S. Reddy, G. Payal, P. Karkulali, M. Himanshu, A. Ukil, and J. Dauwels, "Pressure and flow variation in gas distribution pipeline for leak detection," in *2016 IEEE International Conference on Industrial Technology (ICIT)*, 2016, pp. 679-683.

[5] H. Mishra, P. Karkulali, A. Ukil, and J. Dauwels, "Testbed for real-time monitoring of leak in low pressure gas pipeline," in *IECON 2016 - 42nd Annual Conference of the IEEE Industrial Electronics Society*, 2016, pp. 459-462.

[6] R. S. Reddy, K. Pugalenthi, H. Mishra, A. Ukil, and J. Dauwels, "Anomaly Detection in Low Pressure Gas Distribution Pipeline: Using Pressure and Flow," Unpublished.

[7] A. Hartog,"A distributed temperature sensor based on liquid-core optical fibers," *Journal of Lightwave Technology*, vol. 1, pp. 498-509, 1983.

[8] J. P. Dakin, D. J. Pratt, G. W. Bibby, and J. N. Ross, "Distributed optical fibre Raman temperature sensor using a semiconductor light source and detector," *Electronics Letters*, vol. 21, pp. 569-570, 1985.

[9] F. Tanimola and D. Hill, "Distributed fibre optic sensors for pipeline protection," *Journal of Natural Gas Science and Engineering*, vol. 1, pp. 134-143, Nov 2009.

[10] C. E. Campanella, G. Ai, and A. Ukil, "Distributed fiber optics techniques for gas network monitoring," in textit2016 IEEE International Conference on Industrial Technology (ICIT), 2016, pp. 646-651.

[11] A. Ukil, L. Wang, and G. Ai, "Leak detection in natural gas distribution pipeline using distributed temperature sensing," in *IECON 2016 - 42nd Annual Conference of the IEEE Industrial Electronics Society*, 2016, pp. 417-422.

[12] A. Ukil, H. Braendle, and P. Krippner, "Distributed Temperature Sensing: Review of Technology and Applications," *IEEE Sensors Journal*, vol. 12, pp. 885-892, May 2012.

[13] G. Bolognini and A. Hartog, "Raman-based fibre sensors: Trends and applications," *Optical Fiber Technology*, vol. 19, pp. 678-688, 2013.

[14] H. Su, J. Hu, and M. Yang, "Dam Seepage Monitoring Based on Distributed Optical Fiber Temperature System," *IEEE Sensors Journal*, vol. 15, pp. 9-13, 2015.

[15] J. P. Bazzo, F. Mezzadri, E. V. d. Silva, D. R. Pipa, C. Martelli, and J. C. C. d. Silva, "Thermal Imaging of Hydroelectric Generator Stator Using a DTS System," *IEEE Sensors Journal*, vol. 15, pp. 6689-6696, 2015.

[16] A. V. Tregubov, V. V. Svetukhin, S. G. Novikov, A. V. Berintsev, and V. V. Prikhodko, "A novel fiber optic distributed temperature and strain sensor for building applications," *Results in Physics*, vol. 6, pp. 131-132, 2016.

[17] FEBUS OPTICS, whitepaper. [Online]. Available: http://febus-optics.com/en

[18] A. Motil, A. Bergman, and M. Tur, "[INVITED] State of the art of Brillouin fiber-optic distributed sensing," *Optics & Laser Technology*, vol. 78, Part A, pp. 81-103, 4 2016.

[19] M. Tur, A. Motil, I. Sovran, and A. Bergman, "Recent progress in distributed Brillouin scattering fiber sensors," in *IEEE SENSORS 2014 Proceedings, 2014*, pp. 138-141.

[20] S. Grosswig, E. Hurtig, K. Kuhn, and F. Rudolph, "Distributed fibre-optic temperature sensing technique (DTS) for surveying underground gas storage facilities," *Oil Gas-European Magazine*, vol. 27, pp. 31-34, Dec 2001.

[21] A. A. Khan, V. Vrabie, J. I. Mars, A. Girard, and G. D. Urso, "Automatic Monitoring System for Singularity Detection in Dikes By DTS Data Measurement," *IEEE Transactions on Instrumentation and Measurement*, vol. 59, pp. 2167-2175, 2010.

[22] I. Toccafondo, T. Nannipieri, A. Signorini, E. Guillermain, J. Kuhnhenn, M. Brugger, et al., "Raman Distributed Temperature Sensing at CERN," *IEEE Photonics Technology Letters*, vol. 27, pp. 2182-2185, Oct 15 2015.

[23] Sensornet, Manuals. [Online]. Available: http://www.sensornet.co.uk

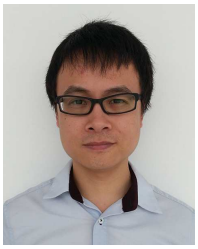

Libo Wang received the B.Eng degree in optical engineering from Zhejiang University, China, in 2007. He also received the Ph.D degree in Materials Science and Engineering from Nanyang Technological University, Singapore, in 2014. From 2008-2013, he was working as a project officer in school of Electrical and Electronic Engineering, NTU. After that, he joined Temasek Laboratories @NTU as a research scientist. Since 2016, he is a research fellow with Energy Research Institute @NTU, working on fiber-optics distributed temperature sensor for gas leak detection. His research interests include optical materials, high power laser system, smart sensors, condition monitoring, data processing and analysis.

Srivathsan Chakaravarthi Narasimman received the B.E. degree in electronics and instrumentation engineering from Anna University, Chennai, India, in 2015 and the M.Sc. degree in computer control and automation from the Nanyang Technological University, Singapore in 2016. Since 2016, he is a Research Associate in the Energy Research Institute at Nanyang Technological University, Singapore. His research interests include process instrumentation, data driven modelling and control theory.

Sugunakar Reddy Ravula received the B.Tech degree in electrical and electronics engineering in 2007 and M.Tech degree in nanotechnolgy in 2009 from Jawaharlal Technological University, Hyderabad, India. He received Ph.D. degree from electrical engineering department, Indian Institute of Technology Madras, Chennai, India in 2015.He is currently working as Research Fellow at Nanyang Technological University, Singapore in advanced multi-sensor anomaly monitoring and analytics for gas pipeline. His research interests include nanomaterials, gas sensors, finite element analysis, condition monitoring, signal processing and data analytics.

Abhisek Ukil (S'05-M'06-SM'10) received the B.E. degree in electrical engineering from the Jadavpur Univ., Kolkata, India, in 2000 and the M.Sc. degree in electronic systems and engineering management from the Univ. of Bolton, Bolton, UK in 2004. He received the Ph.D. degree from the Pretoria (Tshwane) University of Technology, Pretoria, South Africa in 2006, working on automated disturbance analysis in power systems.

From 20062013, he was Principal Scientist at the ABB Corporate Research Center, Baden-Daettwil, Switzerland. Since 2013, he is Assistant Professor in the School of EEE, Nanyang Technological University, Singapore. He is inventor of 10 patents, and author of more than 100 refereed papers, a monograph, 2 chapters. His research interests include condition monitoring, smart grid, renewable energy, signal processing applications.